

8/4/93
E7963

NASA Technical Memorandum 106305

Heat Flux Measurements on Ceramics With Thin Film Thermocouples

Raymond Holanda, Robert C. Anderson, and Curt H. Liebert
Lewis Research Center
Cleveland, Ohio

Prepared for the
SEM Fall Conference Structural Testing Technology at High Temperature
sponsored by the Society for Experimental Mechanics
Ojai, California, November 8-10, 1993

NASA

HEAT FLUX MEASUREMENTS ON CERAMICS

WITH THIN FILM THERMOCOUPLES

Raymond Holanda
NASA Lewis Research Center
21000 Brookpark Road
Cleveland, Ohio 44135

Robert C. Anderson
NASA Lewis Research Center
21000 Brookpark Road
Cleveland, Ohio 44135

Curt H. Liebert
NASA Lewis Research Center
21000 Brookpark Road
Cleveland, Ohio 44135

ABSTRACT

Two methods were devised to measure heat flux through a thick ceramic using thin film thermocouples. The thermocouples were deposited on the front and back face of a flat ceramic substrate. The heat flux was applied to the front surface of the ceramic using an arc lamp Heat Flux Calibration Facility. Silicon nitride and mullite ceramics were used; two thicknesses of each material were tested, with ceramic temperatures to 1500°C. Heat flux ranged from 0.05-2.5 MW/m². One method for heat flux determination used an approximation technique to calculate instantaneous values of heat flux vs time; the other method used an extrapolation technique to determine the steady state heat flux from a record of transient data. Neither method measures heat flux in real time but the techniques may easily be adapted for quasi-real time measurement. In cases where a significant portion of the transient heat flux data is available, the calculated transient heat flux is seen to approach the extrapolated steady state heat flux value as expected.

INTRODUCTION

A survey and analysis of sensor concepts that could be used on ceramic components in advanced propulsion systems was recently carried out^{1,2}. Measurement of surface temperature and heat flux was evaluated in these works and a discussion of the need for further instrumentation development was presented. With the development of advanced propulsion systems, higher hot section temperatures will be encountered. Ceramic components are being developed to withstand these conditions and to avoid the excessive cooling requirements associated with superalloys. Many of these ceramic components will be used without cooling, so that measurement of dynamic heat flux will be of greater interest. However, the use of cooled ceramic components is not precluded, so steady state heat flux measurement is also of interest.

For temperature and heat flux measurement, the attachment of sensors to components is necessary when optical access is not available. Whereas the physical alteration of metallic components is allowable to a certain extent to install sensors, it is usually prohibited on ceramic components because of their brittleness. Thin film thermocouples are one of the very few acceptable contact sensors on ceramics. Not only are they minimally intrusive; they require no physical alteration of the ceramic component and they also exhibit very fast response times. Recent experiments with Pt13Rh/Pt thin film thermocouples on ceramics have demonstrated their use up to 1500 °C in furnace tests on silicon nitride, silicon carbide, mullite, and aluminum oxide³. Experience with high heating rates to temperatures in this range was also demonstrated in reference 3.

An arc lamp Heat Flux Calibration Facility is in use at the NASA Lewis Research Center⁴. It has the capability of generating heat fluxes in the range from 0.03-5.2 MW/m². Thin film thermocouples were deposited on the front and back of flat ceramic specimens and tested in this facility. Two heat flux measurement methods were developed and evaluated in these tests. One method uses an approximation technique to determine instantaneous heat flux at any instant in time from the transient temperature history of the thin film thermocouples. The other method uses an extrapolation technique to estimate the steady state heat flux from the transient temperature history of the thin film thermocouples.

THEORY

Figure 1 is a drawing of a ceramic plate of thickness x at an initial temperature T_0 . Both sides of the plate are instrumented with thin film thermocouples to measure surface temperature. The thermocouple hot junctions are located at the center of the faces of the ceramic. Also shown in figure 1 is a radiative heat source Q_s located on the normal to the hot junctions of the thermocouples. It is assumed that there are no significant temperature gradients in the plane of the plate in this region. When the heat source is turned on, it is assumed that the temperatures of both surfaces of the plate will rise exponentially to final steady state temperatures T_{f1} and T_{f2} according to the relationships

$$\begin{aligned} T_1 &= T_0 + (T_{f1} - T_0) (1 - e^{-c_1 t}) \\ T_2 &= T_0 + (T_{f2} - T_0) (1 - e^{-c_2 t}) \end{aligned} \tag{1}$$

where T = instantaneous surface temperature, T_0 the initial temperature, T_f the final temperature, t = time, and c = time constant. The subscript 1 refers to the ceramic surface near the heat source and the subscript 2 refers to the surface away from the heat source. Conduction and convection of heat to the surrounding gas are assumed to be negligible, and it is also assumed that the plate, as it heats up, is reradiating to an infinite heat sink at T_0 on the back side.

The final steady state temperature difference across the plate approaches $\Delta T_f = T_{f1} - T_{f2}$ as $t \rightarrow \infty$. If the heat source Q_s is extinguished before the steady state condition is reached, the temperature curves may be extrapolated to an estimated steady state condition using functions determined by a curve fit to the form of equation 1.

Assuming isotropic thermal conductivity, the steady state one-dimensional heat flux \dot{Q}_p through the plate may be determined from the relationship

$$\dot{Q}_p = \frac{k}{x} \Delta T_f \quad (2)$$

where k is the thermal conductivity of the ceramic plate. The relationship between the heat flux through the plate and the surface heat flux \dot{Q}_s resulting from the radiative heat source may be expressed as

$$\dot{Q}_p = \alpha_N \dot{Q}_s \quad (3)$$

where α_N is the total absorptance normal to the surface of the ceramic plate.

References 5 and 6 present an analysis of unsteady heat flux sensors. For the case where the transient temperature history of the surfaces of an infinite plate is known, it is shown that the heat flux at any instant of time may be computed as follows:

$$\dot{Q}_p(t) = \frac{k}{x} \left[T_1 \left(t + \frac{x^2}{3\alpha} \right) - T_2 \left(t - \frac{x^2}{6\alpha} \right) \right] \quad (4)$$

where

\dot{Q}_p = one-dimensional heat flux through the plate;

k = thermal conductivity of the plate;

x = plate thickness;

α = thermal diffusivity of the plate;

T_1 = temperature as a function of time at $x = x_1$ (front surface);

T_2 = temperature as a function of time at $x = x_2$ (back surface).

As discussed in reference 6, equation 4 is developed for cyclically varying heat flux values, including single cycles. In this work, the results from reference 6 are applied to a step change in heat flux. Equation 4 is exact for materials whose thermal properties (α and k) do not vary with temperature. In real materials, where property values always vary somewhat with temperature, equation 4 only approximately describes the thermal physics. In this work, when equation 4 is used, the thermal property values used are adjusted during the computation to be suitable for the respective temperatures.

APPARATUS AND TEST PROCEDURE

Test Specimens

Thin film Pt13Rh/Pt thermocouples were fabricated on the front and back faces of silicon nitride and mullite ceramics using the sputtering process. Two test piece sizes with different thicknesses were used: 25x60x3.2 mm, and 25x150x6.4 mm. Silicon nitride is a ceramic with excellent thermal shock capability, and thus can withstand high heat fluxes and large ΔT across the thickness of the test piece. Mullite, on the other hand, has a poor capacity to withstand thermal shock.

A typical test piece is shown in figure 2 placed in a ceramic support fixture. The support fixture is an alumino-silicate ceramic and the test piece slides loosely into a slot in the fixture. The hot junction of the front side thermocouple is located at the center of the test piece and the back side thermocouple hot junction is directly behind it. The thin film thermocouples are 5 μm thick and have a time constant less than 1 msec. Thin-film-to-lead-wire connections are made with 75 μm diameter wire using the parallel gap welding process. The lead wires are insulated with alumina and routed to connectors on the back of the support fixture. A reference thermocouple is mounted on the support fixture. The test piece is shown partially coated with high temperature black paint forming a high absorptance coating on a portion of its surface to increase radiant energy absorptance. Tests were performed with and without the black paint to study the effects of a variation of radiant energy absorptance.

Heat Flux Test Facility

An argon arc lamp Heat Flux Calibration Facility⁴ was used to generate heat fluxes in the range from 0.3-5.2 MW/m². The facility is shown in figure 3a and a closeup view of the arc lamp and sample positioning arm is shown in figure 3b. The calibration function relating steady state heat flux to steady state arc lamp current is shown in figure 4. This data is plotted along with data points obtained using commercially available heat flux gages. The energy of the lamp is focused into a 4x40 mm area with $\pm 1\%$ uniformity, minimizing temperature gradients on the surface of the test piece in this region. Since the thermocouple junction area is small compared to this area of uniform heat flux, this energy uniformity is important to the assumption of one-dimensional heat flow. The facility has a computer-controlled movable arm that moves the test piece into position at the focal plane on command. From the standby condition, the arc lamp attains steady state power level in less than one second. The lamp has a spectral output similar to natural sunlight in the visible region and its spectral output is independent of lamp power. The color temperature of the lamp output is 6500 K.

Because the test duration is short, the data acquisition system in the facility must store all the data from a single test in memory; there is no time to move the data to disk. The data acquisition system for the Heat Flux Calibration Facility has memory sufficient to store 65,000 data points per run. The system can acquire 32,767 data points per channel at the maximum rate of 10,000 Hz. For these experiments three channels were used for each run to record the data from the two thin film thermocouples and a reference thermocouple on the support fixture. Each datum recorded was an average of 10 samples. The system was programmed for averaging to filter out the background noise present in the system.

Figure 5 is a typical graphical output of the Heat Flux Calibration Facility data acquisition system. This graph shows the variation of temperature vs time for the front side and back side thin film thermocouples. The system has taken the voltage data and the "Type R" thermocouple calibration and converted the emf to temperature. Other information shown on the graph is the file number and lamp current. This raw data is then transferred to the data processing software.

Data Processing

Data processing was performed after the test, off line. Data processing was accomplished using PV-WAVE⁷, a workstation data analysis and visualization software package running under the VMS operating system on a Digital Equipment Corp. VAX cluster. The process begins with the reading of the temperature vs time data for the front side and back side thin film thermocouples. The temperature data is assumed to take the form expressed in the following equation which follows the form of equation 1.

$$T = a + b (1 - e^{-ct}) \quad (5)$$

The data processing software performs a fit to the non-linear function of equation 5 using the Gradient-expansion algorithm⁸ which combines the best features of the gradient search with the method of linearizing the fitting function to determine the coefficients a, b, and c for each thermocouple.

Data recording begins when the lamp is turned on and stops soon after the lamp is shut down. This means that there is a lamp startup transient and a lamp shutdown transient included in the data. The software is designed to present the full data to the user so that the user may designate truncation points in order to trim the startup and shutdown transient portions from the data. The software uses only the data within the range selected to determine the coefficients a, b, and c in equation 5. Figure 6 is an example of results from the fitting process. The calculated temperature functions are shown, overplotted with the measured data used for the curve fit. The lamp is shut down before the temperatures reach their asymptotic value either because of data acquisition system storage constraints or to avoid sensor damage caused by excessive temperature. Therefore the actual temperature span available for the curve fit is always a fraction of asymptotic temperature span.

Because the test is aborted before the final steady state temperatures, T_{f1} and T_{f2} , are reached, the final steady state temperature difference, ΔT_f , must be estimated using extrapolation. Extrapolation is carried out using the exponential functions determined in the curve fitting process. Figure 7 is a plot of the extrapolated curves for the two thermocouples. The measured data used in the curve fitting is also plotted on top of the calculated data in figure 7. Figure 8 is a plot of ΔT which results when the two exponential functions are subtracted. The asymptotic value of ΔT (ΔT_f in equation 2) may be used to compute an estimate of the post-transient steady state heat flux using equation 2.

The instantaneous heat flux may also be calculated from the data using equation 4. Calculation of the heat flux at a given time t, using equation 4, requires a value for the front side temperature at a time later than t, and a value for the back side temperature at a time earlier than t. The time shifts are functions of the plate thickness and thermal diffusivity of the material.

The curves shown in Figure 9 typify results from the two methods of heat flux determination used in this work. The straight line represents the heat flux value based on the calculated asymptotic value of ΔT shown in figure 8; and the scattered data represents the instantaneous heat flux calculated using equation 4. In addition, the solid curved line represents the heat flux value assuming, incorrectly, that each value of ΔT on the plot in figure 8 is ΔT_f .

Figure 10 is a plot of the variation of thermal conductivity with temperature provided by the manufacturers for several ceramics, including the silicon nitride and mullite used in these experiments. Figure 11 plots manufacturer's thermal diffusivity data for selected ceramics, also including the materials used in these tests. The significant point to note is the large change in value of these properties with temperature. For this work, empirical equations for thermal diffusivity and thermal conductivity as

functions of temperature were developed using a curve fitting process on manufacturer's data shown in figures 10 and 11.

Equation 4 expresses the instantaneous heat flux as a function of material geometry, time-shifted temperature of the front and back surface, and the thermal conductivity and thermal diffusivity of the material. For calculations using equation 4 in this work, the thermal conductivity value was determined by evaluating the empirical conductivity equation at the temperature halfway between the instantaneous time-shifted temperatures at the front and back surfaces as prescribed by the terms in equation 4. The diffusivity values were determined by evaluating the empirical diffusivity equation at the instantaneous time-shifted temperature associated with the term being evaluated.

Figure 12 is a composite plot of normal total emittance values as a function of temperature for the materials that appear on the surface of the ceramic specimens in the focal area of the arc lamp radiation. The emittance values of the ceramics are from Thermophysical Properties Handbook⁹. Extensive data for alumina was available, but there were few references for silicon nitride, yttria, and silica. The silicon nitride specimens contain 13% yttria and 3% alumina as densification agents. Mullite is made from 60% alumina and 40% silica. The high emittance coating was a commercially available product whose emittance was measured in an experiment at this laboratory. Specimens were tested both with and without the coating to study the effect of variation of energy absorption on test results.

RESULTS AND DISCUSSION

Tests were performed in the Heat Flux Calibration Facility at heat flux levels ranging from 0.3-5.2 MW/m². The temperature of the front and back surfaces of the ceramic test pieces was measured using thin film thermocouples and recorded using the facility data acquisition system. The quantity of data for any given run was limited by the capacity of the data acquisition system and/or the maximum temperature capability of the sensor materials. As a result, the steady state temperature value was never attained. As discussed in the Data Processing section above, figures 5, 6, 7 & 8 show typical results from the data acquisition and extrapolation process. The transient heating curves are assumed to have the functional form of equation 1. The value of ΔT used to compute heat flux by the extrapolation method is defined as the difference, calculated using the fitted curves, between the hot side temperature and cold side temperature in the limit as time $\rightarrow \infty$. For the 85 test runs that were performed in these experiments, the percentage of the asymptotic value of ΔT actually attained ranged from 20-98%.

The large majority of the test runs of these experiments were performed using silicon nitride because of its excellent thermal shock capability. This allowed use of the Heat Flux Calibration Facility over its full range without cracking the test specimen. For the 78 test runs using silicon nitride, the results of the extrapolation method were analyzed to determine what fraction of the heating curve is needed to produce a repeatable determination of the asymptotic value of ΔT . This was done by comparing different tests of the same test piece at several lamp currents. For each lamp current value, the tests were terminated to yield varying percentages of the heating curve. The results of this comparison show that when test runs containing at least 80% of the heating curve were analyzed, the variation in the computed value of ΔT was $\pm 6\%$; test runs containing at least 60% of the heating curve produced a variation in computed ΔT values of $\pm 20\%$. As the available fraction of the heating curve decreases below 60%, the repeatability of the extrapolation deteriorates rapidly. These observations are in general agreement with the conclusions of reference 10 where a similar extrapolation method was used to measure temperature.

The instantaneous one-dimensional heat flux through the test piece, $\dot{Q}_p(t)$, can be computed using equation 4 because the temperature-time history of its front and back surfaces has been directly measured

(see e.g. figure 5). This method is called the approximation method here and offers a good comparison with the extrapolation method and has the additional advantage of being independent of what fraction of the heating curve is available.

Figure 13 is a composite plot of instantaneous one-dimensional heat flux $\dot{Q}_p(t)$ (computed using equation 4) vs hot-side temperature for 21 test runs of the 6.4 mm thick silicon nitride test piece shown in figure 2. While the output of the arc lamp, \dot{Q}_s , is constant for the duration of any single test run, it can be seen that, in general, $\dot{Q}_p(t)$ varies with temperature. This is partially caused by the variation with temperature of the emittance and absorptance of the materials on the surface of the test piece as shown, for example, in figure 12 for the emittance values. The variation of $\dot{Q}_p(t)$ with temperature is also affected by the variation of thermal diffusivity and thermal conductivity with temperature, which was taken into account in the computations made using equation 4.

Equation 3 was used to determine the absorptance variation with temperature for each test run of figure 13 and the results are shown in figure 14. The absorptance was computed as the ratio of the measured instantaneous heat flux from figure 13 to the applied heat flux from figure 4 using knowledge of the lamp current. Figure 14 shows a mean absorptance of 0.45 with a variation of about ± 0.1 . This value of absorptance is seen to be intermediate to the emittance values of the various materials on the surface of the test specimens: i.e., the sensor materials, the coating, and the ceramics (figure 12).

Similar tests to determine α_N were also performed using a 3.2 mm thick silicon nitride specimen shown in figure 15. Fifty tests were performed using this test piece: 15 tests with no coating; 30 tests with a partial coating of a high emittance material, as shown in figure 15; and 5 tests with a fully coated specimen. For this fully coated specimen the coating extended over the thin film thermocouple junction in the region of the focal area of the lamp. Instantaneous heat flux values were computed, using equation 4, and the corresponding values of absorptance were determined for the three surface coating configurations. The shadow bands of this absorptance data are shown in figure 16. The mean absorptance values were 0.28 for the uncoated specimen, 0.42 for the partially coated specimen, and 0.62 for the fully coated specimen.

Since the values of absorptance and emittance are functions of surface properties only it would be expected that the absorptance variation vs temperature would be in agreement for similar surface characteristics regardless of specimen thickness. This is found to be true for the results from the partially coated specimens of figures 2 and 15 which are in close agreement.

Tests were performed in the Heat Flux Calibration Facility using uncoated mullite ceramic test specimens. These test pieces were instrumented with thin film thermocouples and mounted in the facility in exactly the same manner as the silicon nitride. Mullite's distinguishing thermal property in this application is its poor thermal shock capability. This causes the mullite to crack with a ΔT as low as 100°C between the front side and back side of the test piece, even at the lowest applied heat flux level of 0.3 MW/m^2 . The consequence of this problem was that only a small portion of the heating curve could be generated for any test run. The extrapolation method was therefore not applicable to this material, pointing out the major shortcoming of this method. The approximation method was successfully used to measure heat flux through the mullite. Emittance was calculated to be 0.37. With lower heat flux levels larger percentages of heating curves would be available; but this facility has a lower threshold limit at 0.3 MW/m^2 caused by the necessity to maintain the stability of the arc. (Since this work was done, a method has been devised to push the lower threshold steady state heat flux to 0.03 MW/m^2 .)

Accuracy Considerations

An analysis was performed to estimate the accuracy of the heat flux values computed by the extrapolation and approximation technique. Results of an error analysis for the Heat Flux Calibration Facility were presented in ref. 4, which estimated the uncertainty in the heat flux value for the calibration system to be $\pm 7\%$. Primary sources of error were the repeatability of the arc lamp intensity, the variability of the positioning system, and electrical noise in the data acquisition system.

For the present work the uncertainty in the values for ceramic thermal conductivity and thermal diffusivity was estimated to be $\pm 10\%$. These property values were provided by material manufacturers and are likely based on statistical results from a sampling program. Emittance values shown in figure 12, which are handbook values rather than values provided for the specific material used, have an uncertainty of about $\pm 20\%$. It was necessary in this work to extrapolate the material properties to higher temperatures than provided by the manufacturers. This adds an additional uncertainty to these values.

The curve fitting process used in the extrapolation method was seen to determine the asymptotic heat flux values with an overall variation of $\pm 6\%$ when at least 80% of the heating curve was available. A gradual increase in overall variation was seen as the amount of available heating curve diminished. The accuracy of sputtered thin film thermocouples was evaluated³ and determined to be about $\pm 3\%$.

An error in heat flux computation occurs for both the extrapolation and approximation method because the surrounding temperature is not maintained at a constant value throughout the experiment. The support fixture heats up during a test run from stray radiation from the arc lamp. Because the support fixture has large mass compared to the test specimen and is not situated in the focal area of the lamp, the effect is not large. It was calculated to cause $\leq 5\%$ reduction in heat loss from the test piece compared to a test piece in an isothermal environment throughout the experiment.

Mathematically, heat flux values computed by the extrapolation technique and the approximation technique should converge as the available heating curve approaches 100% of its value. This agreement was found to be within 5% for tests where the available heating curve was greater than 70%.

For this work it was assumed that the ceramic materials were opaque. It was also assumed that there were no convection effects in the area surrounding the test piece. These assumptions are considered to introduce no significant errors in the conclusions of this report.

The assumption of one-dimensional heat flow was based on the fact that the area of maximum energy from the arc lamp has a $\pm 1\%$ uniformity of energy over a rectangular area of 4x40 mm on the front face of the test piece, and the thin film thermocouple hot junction is small and is located at the center of this area. However, because of the finite thickness of the test pieces, the heat transfer by conduction through the test piece is three-dimensional; the diffusion of heat from any point on the front surface proceeds according to a cosine distribution. The use of test pieces of 2 different thicknesses with the same coating showed heat flux that averaged 7% greater for the thicker test piece at the same applied heat flux. This could be explained by a proportionately cooler back-side thermocouple temperature for the thicker test piece resulting from diffusion of heat to larger areas of the back surface.

Another aspect of the one-dimensional heat flow assumption can be investigated by comparing the same test piece in the uncoated and partially coated configuration. From figure 15, it is seen that the partial coating is applied within about 1 mm of the thermocouple junction. A comparison of the heating curves of the hot side thermocouple for the same applied heat flux in these two configurations showed a significantly higher temperature throughout any test run for the coated configuration, demonstrating two-

dimensional heat flow even at the front surface of the test piece. The effect this has on the tests is that the emittance and absorptance properties of the front surface of the test piece are more accurately represented by the composite effects of all the materials on the surface (sensor, ceramic, and coatings), rather than just the sensor material itself. But since the energy from the lamp is constant within $\pm 1\%$ over a 4 x 40 mm area surrounding the sensor hot junction, no significant error should result from this effect.

The net effect of all the uncertainties discussed here is difficult to estimate because some effects are offsetting while others are additive. The root mean square of these errors is estimated to be in the range of $\pm 15\text{-}30\%$ uncertainty in heat flux accuracy.

To add credence to the experimental results, the method of reference 11 was used to determine surface heat flux for comparison with the results of this work. The method of reference 11 is only useable at early heating times when the front side temperature is changing rapidly and requires knowledge of the derivative of the temperature vs time function as it varies through the specimen along a line normal to the surface. For this comparison, the temperature and the derivative of temperature with respect to time were assumed to vary linearly through the test piece. The two values compared were 1) a 2.5 second average heat flux from the reference 11 calculation beginning after the first .5 seconds of data and 2) an average equation 4 heat flux over a short time duration starting at the beginning of available equation 4 data.

The average percent difference between the two values for 38 tests was a highly acceptable 24% with a standard deviation of 9%.

CONCLUDING REMARKS

Two methods for heat flux determination on thick ceramic substrates using Pt13Rh/Pt thin film thermocouples were evaluated. An argon arc lamp Heat Flux Calibration Facility was used to generate known heat fluxes in the range from 0.3-5.2 MW/m². The approximation method was used to calculate instantaneous values of heat flux vs time. The extrapolation method was used to compute steady state heat flux from transient data.

Theory and analysis was presented to describe the basis of each approach for computing heat flux. The calibration system was described; its accuracy had been determined to be about $\pm 7\%^4$. Silicon nitride and mullite ceramics were used. Two thicknesses of each material were used, with ceramic temperatures to 1500°C on the silicon nitride.

Results were presented using the extrapolation method to show that 60% of the heating curve was needed to produce variation of computed heat flux values within $\pm 20\%$. With 80% or more of the heating curve, variation was reduced to $\pm 6\%$. The comparison of the approximation and extrapolation methods showed agreement to $\pm 5\%$ with heating curves $\geq 70\%$. Variation of material properties with temperature was incorporated in the computations.

Analysis of the validity of assumptions concerning the heat transfer model for the experiments was assisted by the use of two thicknesses of ceramic specimen, three configurations of energy absorptive properties of the surface of the ceramic, and measurement of the support structure temperature variation. Overall accuracy of the experiments was estimated to be between ± 15 and $\pm 30\%$.

ACKNOWLEDGEMENTS

The authors acknowledge the invaluable assistance of Gerald A. Danzey in the fabrication of the test specimens, and William T. Dedula and George W. Readus Jr. in the operation of the heat-flux calibration facility.

REFERENCES

1. Bennethum, W. H.; and Sherwood, L. T.: Sensors for Ceramic Components in Advanced Propulsion Systems. NASA CR-180900, Aug. 1988.
2. Atkinson, W. H.; Cyr, M. A.; and Strange, R. R.: Development of Sensors for Ceramic Components in Advanced Propulsion Systems. NASA CR-182111, June, 1988.
3. Holanda, R.: Development of Thin Film Thermocouples on Ceramic Materials for Advanced Propulsion System Applications. Seventh International Symposium On Temperature: Its Measurement and Control in Science and Industry. Toronto, Canada, Apr. 1992.
4. Liebert, C.; and Weikle, D. H.: Heat Flux Measurements. NASA TM-101428, 1989.
5. Baines, D. J.: A Comparative Theoretical Evaluation of Five Commonly Used Types of Heat Flux Sensors. Report HSA 27, 1970.
6. Jepps, G. : Heat Conduction in Single-Layer and Double-Layer Walls, with Boundary Conditions Appropriate to Aerodynamic Heating, Report ACA-66, November 1965.
7. Precision Visuals Inc., **PV-WAVE Technical Reference Manual**, Version 3.0, August 1990.
8. Bevington, P. R.: **Data Reduction and Error Analysis for the Physical Sciences**. McGraw-Hill, New York, 1969.
9. Touloukian, Y. S.; and DeWitt, D. P.: **Thermophysical Properties of Matter**. Vol. 8, Thermal Radiative Properties- Nonmetallic Solids, 1972.
10. Glawe, G. E.; Will, H. A.; and Krause, L. N.: A New Approach to the Pulsed Thermocouple for High Gas Temperature Measurements. NASA TM X-71883, 1976.
11. Liebert, C.H.: Miniature High Temperature Plug-Type Heat Flux Gauges. NASA TM 105403, 1992.

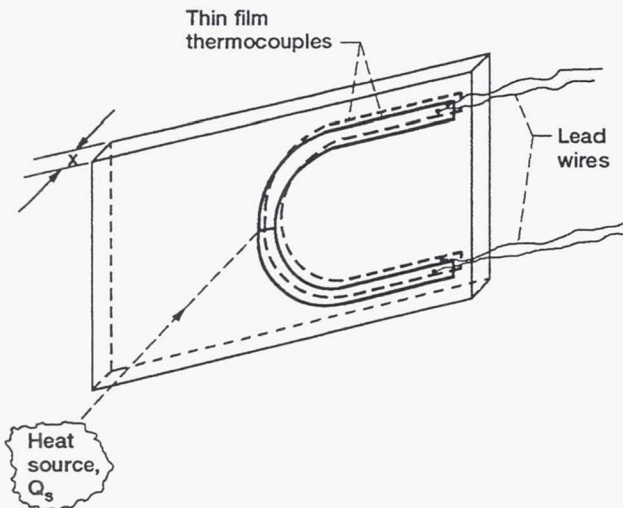


Figure 1.—Schematic drawing of ceramic test specimen in Heat Flux Calibration Facility.

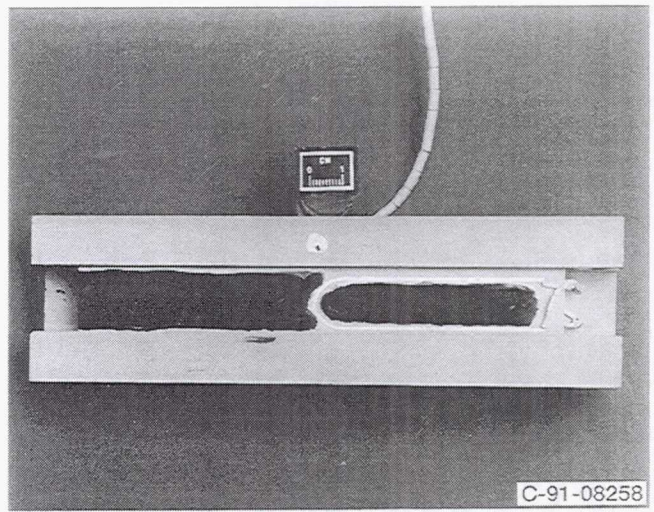
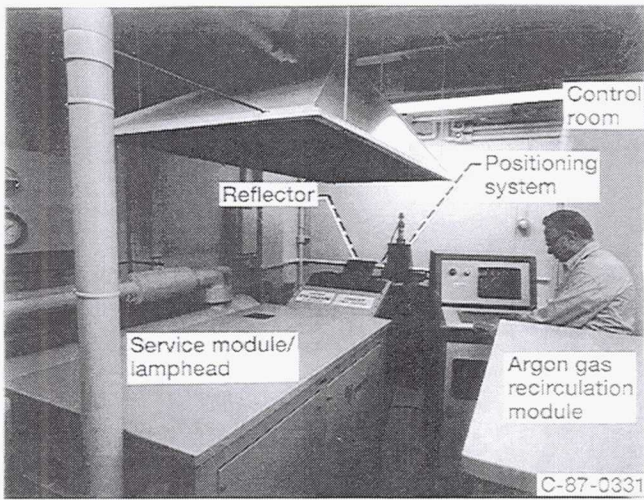
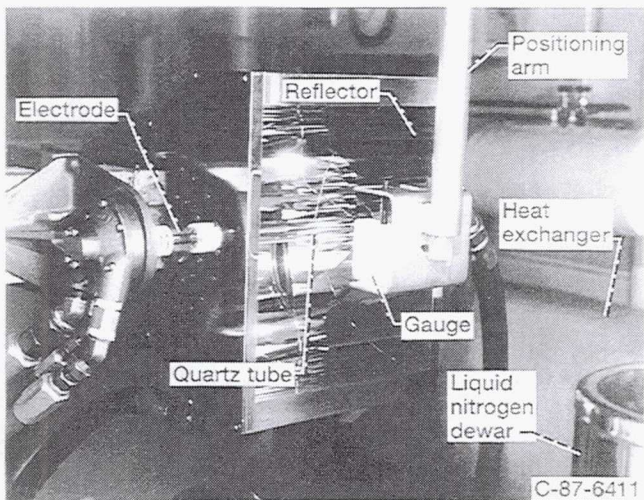


Figure 2.—Silicon nitride test specimen, 6.4 mm thick, with thin film thermocouples, lead wires, support fixture, and high-emittance coating.



(a) Heat Flux Calibration Facility.



(b) Facility arc lamp and positioning arm.

Figure 3.—Argon Arc-Lamp Heat Flux Calibration Facility.

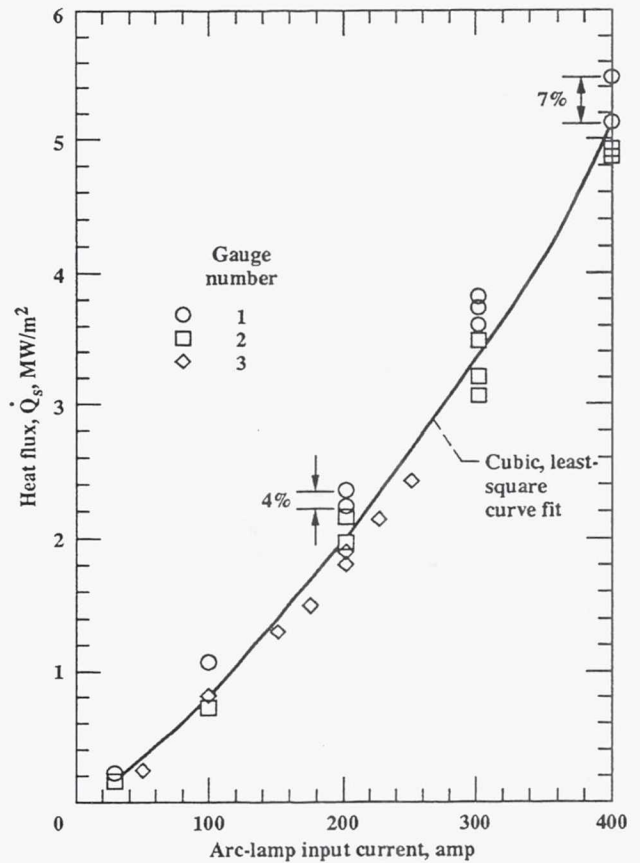


Figure 4.—Calibration curve for Heat Flux Calibration Facility.

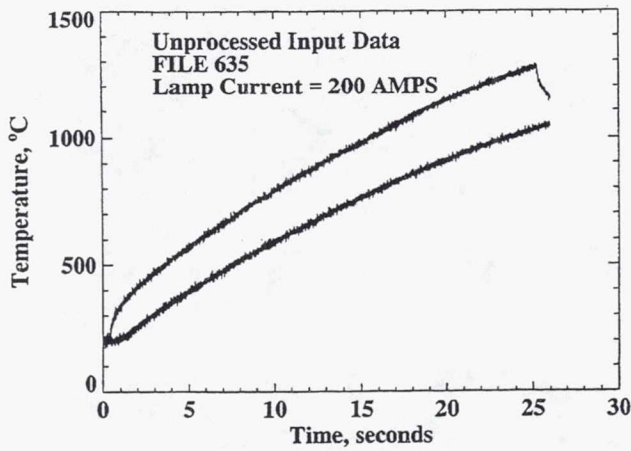


Figure 5.—Typical output of thin film thermocouples on ceramic test specimen as produced by facility data acquisition system.

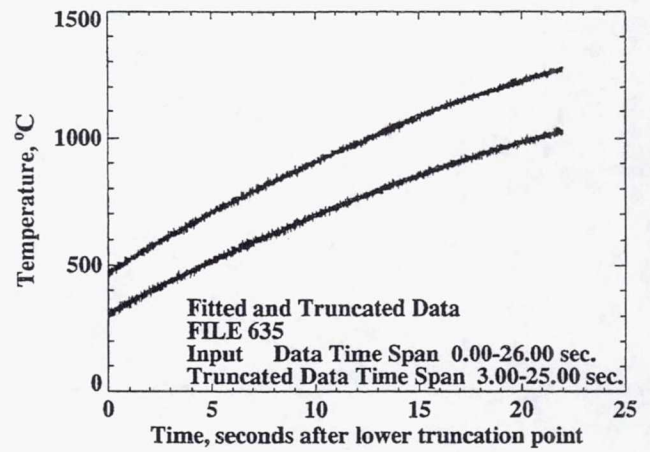


Figure 6.—Thin film thermocouple output data shown truncated and overlplotted with calculated temperature functions.

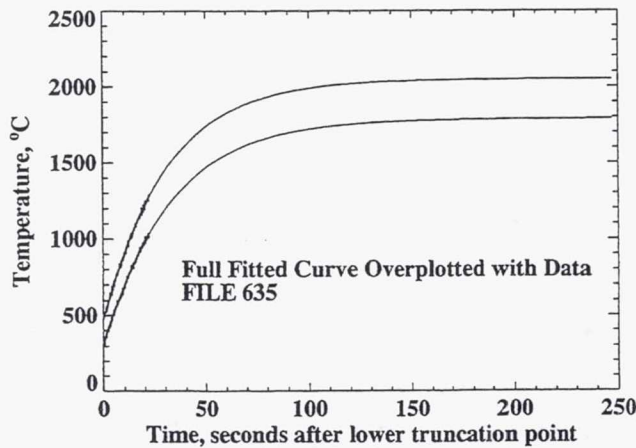


Figure 7.—Full extrapolated thin film thermocouple temperature functions overlplotted with actual output data.

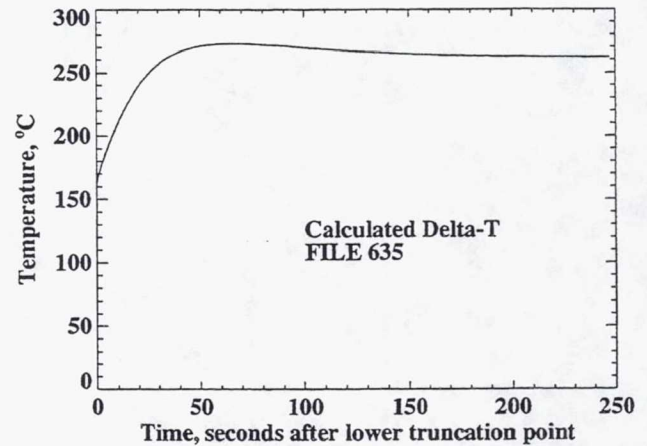


Figure 8.—Plot of ΔT curve obtained from calculated and extrapolated thin film thermocouple temperature functions, including ΔT_f value.

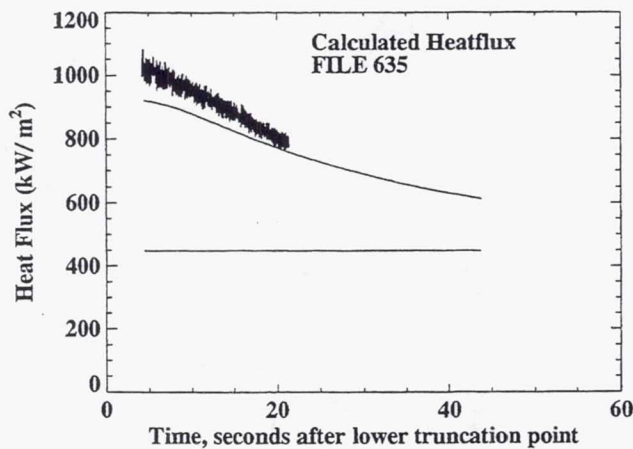


Figure 9.—Heat flux values obtained from extrapolation method (straight line and curved line) and approximation method (scattered data).

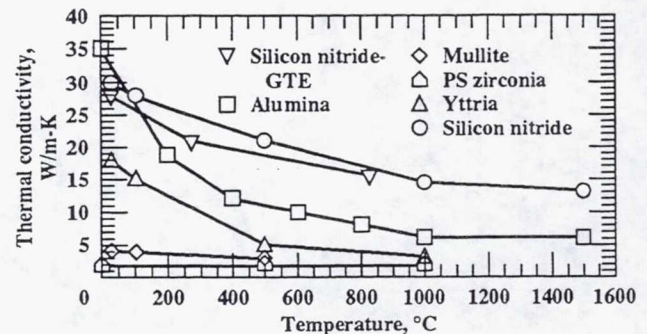


Figure 10.—Thermal conductivity of selected ceramics.

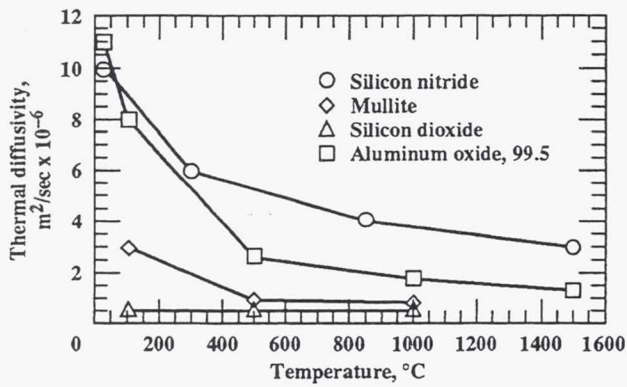


Figure 11.—Thermal diffusivity of selected ceramics.

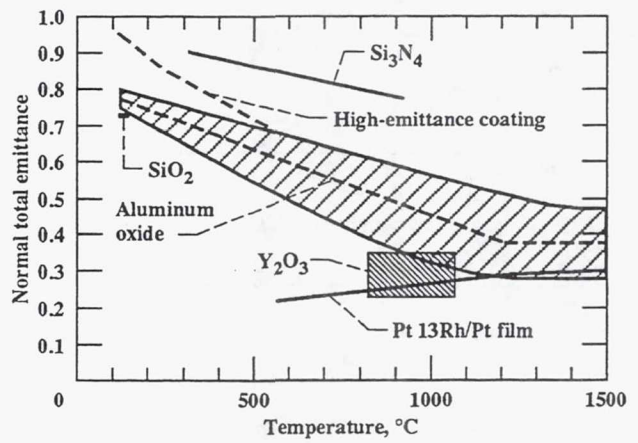


Figure 12.—Normal total emittance values for the materials on the surface of the test specimens.

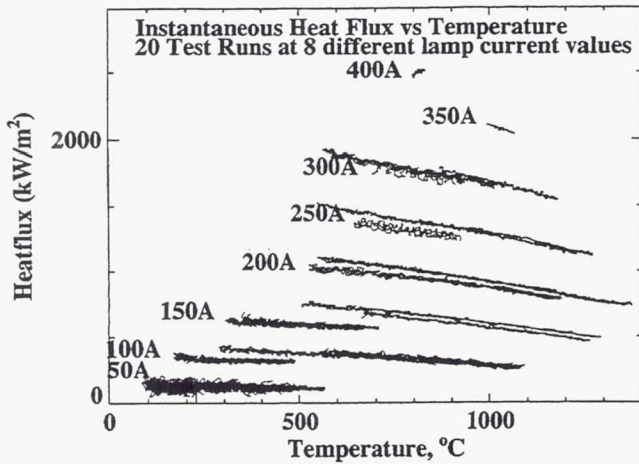


Figure 13.—Instantaneous heat flux versus temperature at several arc lamp currents for 6.4 mm thick silicon nitride test specimen shown in figure 2.

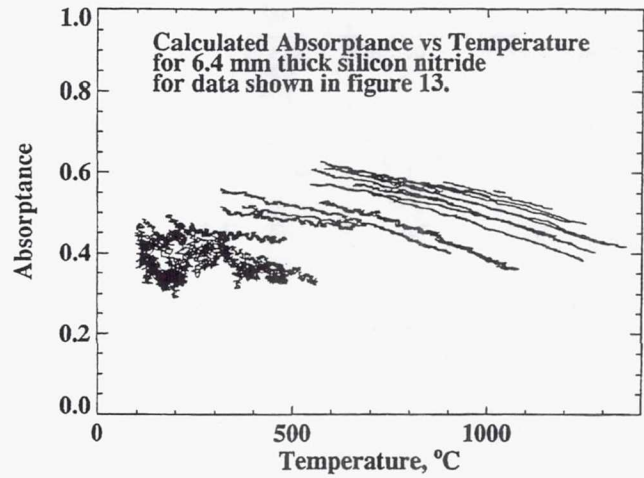


Figure 14.—Absorptance versus temperature values for 6.4 mm thick silicon nitride test specimen shown in figure 2, for data shown in figure 13.

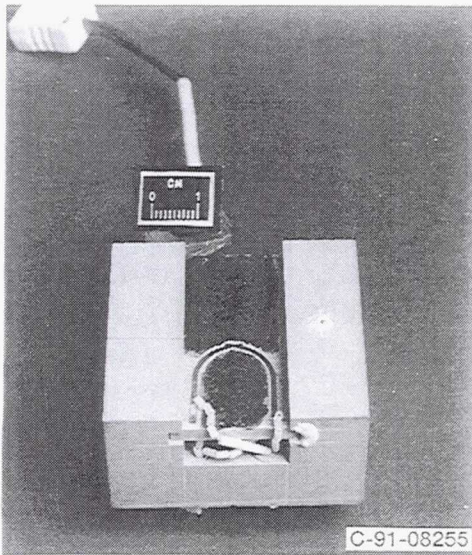


Figure 15.—Silicon nitride test specimen, 3.2 mm thick, with thin film thermocouples, lead wires, support fixture, and high-emittance coating.

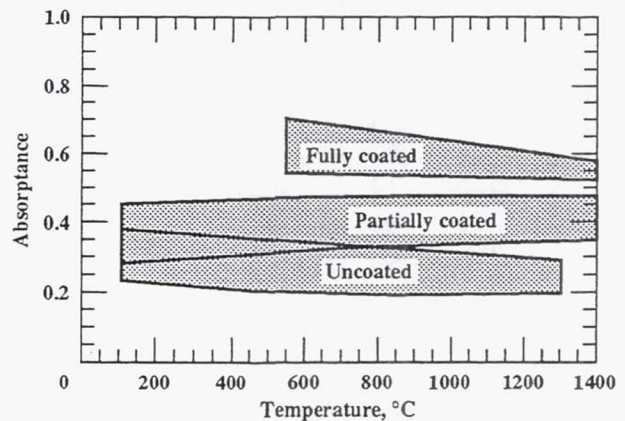


Figure 16.—Absorptance versus temperature values for 3.2 mm thick silicon nitride test specimen shown in figure 15.

REPORT DOCUMENTATION PAGE

Form Approved
OMB No. 0704-0188

Public reporting burden for this collection of information is estimated to average 1 hour per response, including the time for reviewing instructions, searching existing data sources, gathering and maintaining the data needed, and completing and reviewing the collection of information. Send comments regarding this burden estimate or any other aspect of this collection of information, including suggestions for reducing this burden, to Washington Headquarters Services, Directorate for Information Operations and Reports, 1215 Jefferson Davis Highway, Suite 1204, Arlington, VA 22202-4302, and to the Office of Management and Budget, Paperwork Reduction Project (0704-0188), Washington, DC 20503.

1. AGENCY USE ONLY (Leave blank)	2. REPORT DATE November 1993	3. REPORT TYPE AND DATES COVERED Technical Memorandum	
4. TITLE AND SUBTITLE Heat Flux Measurements on Ceramics With Thin Film Thermocouples		5. FUNDING NUMBERS WU-505-62-50	
6. AUTHOR(S) Raymond Holanda, Robert C. Anderson, and Curt H. Liebert		7. PERFORMING ORGANIZATION NAME(S) AND ADDRESS(ES) National Aeronautics and Space Administration Lewis Research Center Cleveland, Ohio 44135-3191	
8. PERFORMING ORGANIZATION REPORT NUMBER E-7963		9. SPONSORING/MONITORING AGENCY NAME(S) AND ADDRESS(ES) National Aeronautics and Space Administration Washington, D.C. 20546-0001	
10. SPONSORING/MONITORING AGENCY REPORT NUMBER NASA TM-106305		11. SUPPLEMENTARY NOTES Prepared for the SEM Fall Conference Structural Testing Technology at High Temperature sponsored by the Society for Experimental Mechanics, Ojai, California, November 8-10, 1993. Responsible person, Raymond Holanda, (216) 433-3738.	
12a. DISTRIBUTION/AVAILABILITY STATEMENT Unclassified - Unlimited Subject Category 35		12b. DISTRIBUTION CODE	
13. ABSTRACT (Maximum 200 words) Two methods were devised to measure heat flux through a thick ceramic using thin film thermocouples. The thermocouples were deposited on the front and back face of a flat ceramic substrate. The heat flux was applied to the front surface of the ceramic using an arc lamp Heat Flux Calibration Facility. Silicon nitride and mullite ceramics were used; two thicknesses of each material was tested, with ceramic temperatures to 1500°C. Heat flux ranged from 0.05-2.5 MW/m ² . One method for heat flux determination used an approximation technique to calculate instantaneous values of heat flux vs time; the other method used an extrapolation technique to determine the steady state heat flux from a record of transient data. Neither method measures heat flux in real time but the techniques may easily be adapted for quasi-real time measurement. In cases where a significant portion of the transient heat flux data is available, the calculated transient heat flux is seen to approach the extrapolated steady state heat flux value as expected.			
14. SUBJECT TERMS Thermocouple; Thin film; Heat flux; Ceramics		15. NUMBER OF PAGES 14	
		16. PRICE CODE A03	
17. SECURITY CLASSIFICATION OF REPORT Unclassified	18. SECURITY CLASSIFICATION OF THIS PAGE Unclassified	19. SECURITY CLASSIFICATION OF ABSTRACT Unclassified	20. LIMITATION OF ABSTRACT

National Aeronautics and
Space Administration

Lewis Research Center
Cleveland, Ohio 44135

FOURTH CLASS MAIL

ADDRESS CORRECTION REQUESTED



Official Business
Penalty for Private Use \$300

NASA
